Stimulation and Binding Properties of Polyelectrolyte Multilayers Verified by ATR-FTIR Spectroscopy

Martin Müller, Susanne Heinen, Ulrich Oertel, Klaus Lunkwitz*

Institute for Polymer Research Dresden e.V., D-01069 Dresden, Germany

SUMMARY: We report on the deposition and properties of multilayers composed of reactive polymers on planar surfaces. As reactive polymers the polycations poly(ethylene-imine), poly(L-lysine) (PLL), poly(allylamime) (PAA) and the polyanions poly(acrylate) (PAC), poly(vinylsulfate), poly(maleate-co-olefines) were used. ATR-FTIR spectroscopy was adopted to study deposition, binding and stimulation properties of polymer multilayers. The binding of charged species of different molecular size such as rhodanide anions and sodium oleate from solution was examined, whereby binding was found to be dependent on the charge of the outermost layer. For these two analytes a selectivity parameter Q, defined as the ratio between the adsorbed amount obtained at the negatively charged and that at the positively charged surface, respectively, was determined. Furthermore, swelling experiments on multilayer assemblies of PLL and PAC exposed to mixtures of ethanol/water (10 - 70% EtOH content) were carried out. Our experiments gave evidence, that the PLL layers showed a more significant increase in density than the PAC layers. The conformation of PLL incorporated into multilayers could be changed by pH variation.

INTRODUCTION

Beside the surface modification concept of self assembled monolayers (SAM) of amphiphilic molecules consisting of a hydrocarbon part and a chemoreactive anchor group typically trichloro- or trialkoxysilane,[1, 2] sulfhydryl[3] or phosphonate,[4] a novel concept has been initiated by Decher,[5] which makes use of the consecutive adsorption of oppositely charged polyelectrolytes. By this electrostatic self assembly (ESA) concept[6] polyelectrolyte multilayers systems (MLS) are generated, which provide for coatings of defined and controlled thickness as well as morphological and chemical surface homogeneity. We were interested in two particular aspects of multilayer systems, i.e their swelling properties (i) and their surface selectivity via the outermost layer (ii), which is schematically shown in Fig. 1. Concerning to the latter (ii) one important application field for us has been the design of bioinert surfaces, aiming at the prevention of protein adsorption at relevant medical or food processing devices, container materials or tubing in contact with biological fluids via the last adsorbed layer.[7-9] In analogy to proteins we report here on the adsorption of molecular smaller

© WILEY-VCH Verlag GmbH, D-69469 Weinheim, 2001 CCC 1022-1360/00/$ 17.50+.50/0

charged species like rhodanide and surfactants (oleate). Furthermore concerning to (i), multilayers have interesting application fields for the functional membrane modification, especially for the separation of water/organic solvent mixtures in pervaporation membranes.[10] Therefore we exposed multilayer systems to mixtures of ethanol/water studying the selective swellability in the whole multilayer assembly. Finally, the pH induced switching of polyelectrolyte multilayers containing PLL as a polycation is reported.

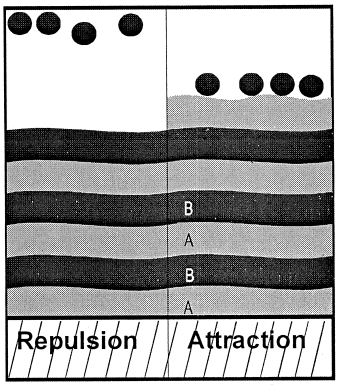

Fig. 1. Surface selectivity of multilayer systems determined by the outermost polyelectrolyte layer (grey layers are positively, black layers and adsorbates are negatively charged, respectively.

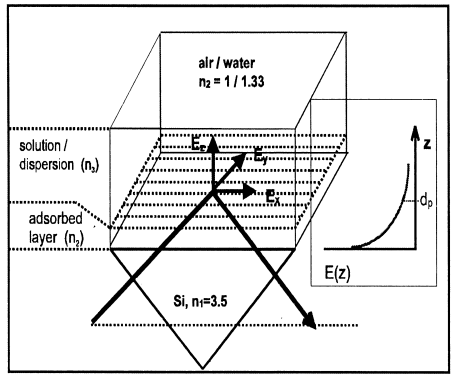

Fig. 2. Scheme of the ATR-FTIR principle

As analytical method the surface and layer sensitive *in-situ*-ATR-FTIR-Spectroscopy,[11, 12] whose principle is given in Fig. 2, was chosen enabling *on-line* control of the multilayer deposition on the molecular level and further the quantitative determination of the adsorption of different analytes from solution at the multilayer surface.

EXPERIMENTAL PART

Surfaces

As model surfaces for the polyelectrolyte multilayer modification plasma cleaned (plasma chamber PDC-32G, Harrick, 1 Torr, 2 min, 100W) Internal Reflexion Elements (IRE) of Si ($n_1 = 3.5$) were used.

Polyelectrolytes, chemicals

Poly(acrylic acid) (PAC, Sigma, M_w = 90.000) was used without further preparation. The sodium salt of poly(maleic acid-co-α-methylstyrene) (PMA-MS) was obtained by refluxing poly(maleic anhydride-co-α-methylstyrene) (Mw = 23.000, Leuna) in water in the presence of a twofold excess of sodium hydroxide. Poly((3-(N,N-dimethylamino)-propyl)maleimide-co-α-methylstyrene) (PMI-MS) was synthesized by polymer analogous reaction of PMA-MS with N,N-dimethylaminopropylamine.[13] Poly(diallyldimethylammonium chloride) (PDADMAC, linear, M_w = 160.000, W. Jaeger, Fraunhofer Institut für Angewandte Polymerforschung) and branched poly(ethyleneimine) hydrochloride (PEI, Aldrich, M_W = 750.000) was used as delivered. All polyelectrolytes were dissolved in deionized water (Millipore, 18.2 MΩ) to a concentration of 0.005 – 0.01m. Sodium rhodanide was from Riedel de Haen and the sodium salt of oleic acid (oleate) was purchased from Sigma.

Multilayers

The multilayers of oppositely charged polyelectrolytes were fabricated by consecutively exposing the Si IRE to polycation and polyanion solutions in the sample compartment of the ATR-FTIR sorption cell (IPF Dresden) according to the stream coating procedure described therein[7]. Between every polyelectrolyte addition, the sorption cell was carefully rinsed with water.

ATR-FTIR-Spectroscopy

The *in-situ-ATR-FTIR Apparatus for Sorption Measurements* (U. P. Fringeli, University of Vienna, OPTISPEC, Zürich), consisting of a special mirror setup and the *in-situ*-sorption cell (IPF Dresden) was used on a commercial FTIR-spectrometer (IFS 28, BRUKER) equipped with globar source, MCT detection and rapid scan option, as described elsewhere.[7, 8] ATR-FTIR absorbance spectra were recorded by the SBSR-(Single Beam-Sample Reference)-method, whereby single channel spectra I and I_0 were recorded of both the upper (I) and lower (I_0) half of the Si-IRE (50*20*2 mm^3). Above the sample and reference half are two liquid chambers (I, I_0) sealed by O-rings, which are filled with polyelectrolyte or protein solution (S-chamber) and with water (R-chamber), respectively. Ratioing of the single channel spectra according to $A_{SBSR} = -\log (I/I_0)$ resulted in absorbance spectra (A_{SBSR}), which exhibited a proper compensation of the background absorptions due to the SiO_x-layer, the solvent (water), the water vapor (spectrometer) and ice on the MCT detector window.

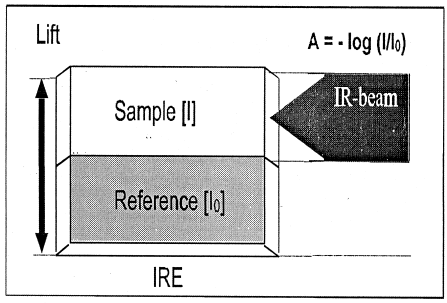

Fig. 3. Scheme of the SBSR principle (see text).

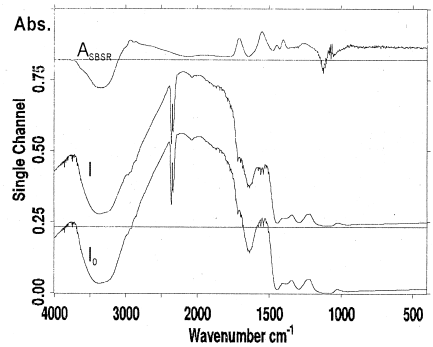

Fig. 4. Typical A_{SBSR}-(absorbance) spectrum of a PEI/PAC multilayer (top) computed by I/I_0, whereby I and I_0 denote the corresponding single channel intensity spectrum of the upper (MLS-PEI/PAC-6, Si, H_2O) and lower IRE half (Si, H_2O), respectively.

Swelling experiments

ATR-FTIR spectra were recorded after alternately depositing 20 layers of PLL and 20 layers of PAC in H_2O. The multilayer in sample compartment was then exposed to EtOH/H_2O mixtures. The respective mixture was also filled in the reference chamber.

RESULTS AND DISCUSSION

Deposition of Polyelectrolyte Multilayers

The Polyelectrolyte multilayer deposition on plasma treated Si IREs was monitored by *in-situ* ATR-FTIR-spectroscopy as it was initally described therein[7]. Here we show the alternate layer built up of PLL and a copolymer of maleic acid, i.e. the poly(maleic acid-co-α-methylstyrene) (PMA-MS), which is an additional suitable carboxyl containing weak polyanion. Concerningly, in Fig. 5 ATR-FTIR spectra are shown (from bottom to top), which were recorded after every adsorption step of the two polyelectrolyte components PLL and PMA-MS at the SiO_x surface. For comparison the IR spectra of the single components are

shown on the top. An assignment of the relevant IR bands is given in Table 1. Especially, for the center wavenumber of the $\nu_a(COO^-)$ band we observed a significant deviation for the single bulk PMA-MS and for PMA-MS incorporated in the multilayers, which might be attributed to the complex formation between the carboxylic and the ammonium groups.

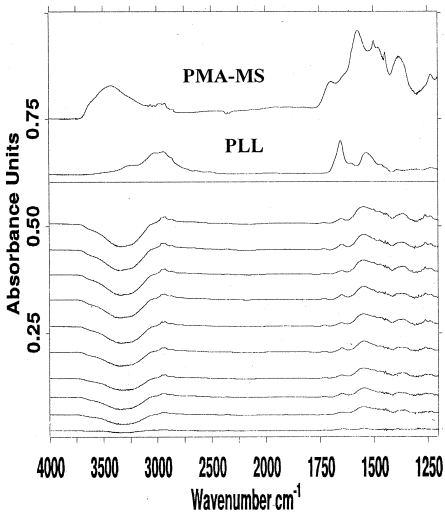

Fig. 5. Lower part (from bottom to top): *in-situ*-ATR-FTIR-spectra monitoring the alternate deposition of PLL and PMA-MS after the adsorption steps 1 to 10, respectively, at the Si-IRE (n_1=3.5, incident angle θ= 45°, 11 active reflexions). Upper part: bulk IR spectra of PLL and PMA-MS.

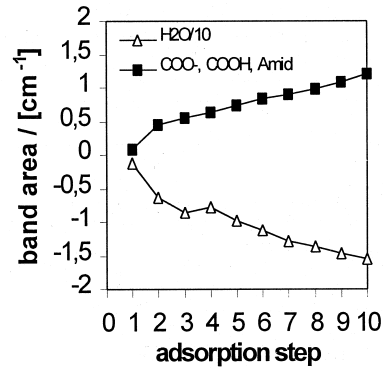

Fig. 6. Integrated areas of the ν(OH) (scaled by 0.1), and the composed band consisting of the $\nu(COO^-)$, Amide I and ν(C=O) refering to the multilayer ATR-FTIR spectra in Fig. 5 in dependence on the adsorption step (PLL: odd steps, PMA-MS: even steps).

For the on-line monitoring of multilayer formation we used the total area of the overlapped bands of the ν(CO) (COOH groups) at 1695 cm^{-1}, the amide I at about 1650 cm^{-1} and the $\nu_a(COO^-)$ (COO^- groups) at 1575 cm^{-1} of PMA-MS within the spectral range from 1750 – 1425 cm^{-1}. In Fig. 6 the integrated areas of these bands are plotted against the adsorption step, proving the layer growth by the increase of the $\nu_a(COO^-)$. Additionally, we observed an increase of the negative ν(OH)-band (3700-3100 cm^{-1}) of water, since by layer growth the neighboring water/solid interface in the sample compartment was subsequently moved away

from the substrate surface in comparison to the unmodified surface in the reference compartment, as it was shown previously.[7)]

Table 1. Assignment of the infrared bands of the polyelectrolyte components in PLL/PMA-MS multilayers

wavenumber / [cm^{-1}]	assignment	component
3700-3100	ν(OH)	water
1695 (+/-5)	ν(C=O)	PMA-MS
1645 (+/-)	Amide I	PLL
1570 (+/-10)	$\nu_a(COO^-)$	PMA-MS
1370 (+/-10)	$\nu_s(COO^-)$	PMA-MS

Swelling properties of multilayer systems

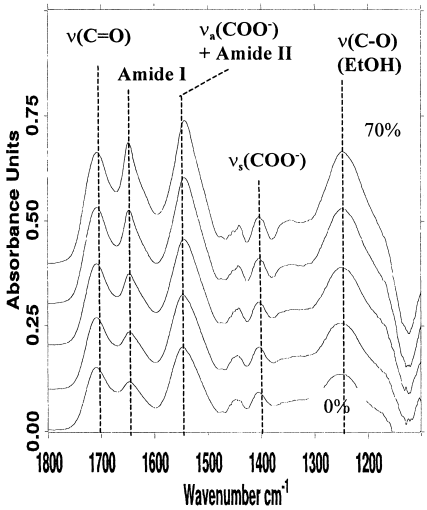

Fig. 7. ATR-IR-spectra of PLL/PAC-MLS in contact to 0, 10, 30, 50, 70 % EtOH-water-mixtures (bottom to top). The IR marker bands of the PLL and PAC layers are indicated

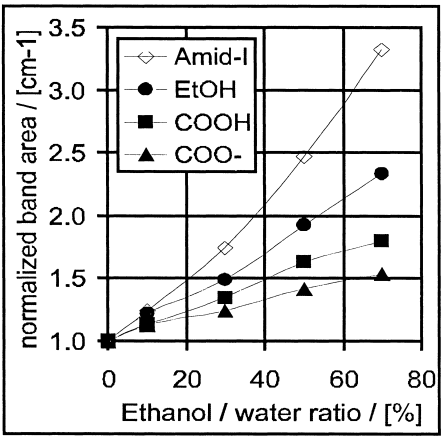

Fig. 8. Plot of the normalised areas (A/A_0) of IR-bands corresponding to the partial poly-electrolyte layers in dependence of the EtOH content. Every PEL band A was normalised by the respective band, measured in the presence of pure water (A_0).

Materials, which are selectively swellable by either organic or aqueous solvents are of highly practical relevance. Since composite membranes based on polyelectrolyte multilayer assemblies have been reported for the separation of water/alcohol mixtures,[10] we were interested in the response of multilayer systems exposed to different ETOH/H_2O mixtures. For that we have chosen a rather thick multilayer system of PLL/PAC (d > 1μm), which was fabricated by 20 PLL and 20 PAC alternate adsorption cycles, as a model system. Both PLL and PAC have intense characteristic IR bands, which alter there intensity upon swelling. Concerningly in Fig. 7, *in-situ* ATR-FTIR spectra of the MLS-PLL/PAC-40 on a Si IRE, are shown, which were recorded during the exposition to pure water (0%, bottom) and subsequently to mixtures of EtOH/water of 10, 30, 50 and 70% (top) EtOH content.The integrated areas of the ν(C=O) and the ν(COO^-) bands of carboxylic acid and carboxylate groups of the PAC component as well as of the Amide I band due to the PLL component were normalized by the respective IR bands of the multilayer spectrum recorded in the presence of pure water and are plotted against the experimental EtOH content in Fig. 8. Additionally, the ν(C-O) of EtOH is plotted, which seems to be approximately linear to the EtOH content. For the course of the normalized polycation and polyanion IR bands in dependence of the EtOH content we can not give a rigorous quantitative analysis here. However, it should be mentioned that there is unambigous relevance for swelling, if the integrated band area of a swellable polyelectrolyte layer is *decreasing* with respect to the initial state, since the concentration c is also decreasing by partial dissolving of polymer segments according to the equation (1).

$$A = \varepsilon \, c \, d_e(d) \qquad (1)$$

Thereby A, ε and d_e are the integrated absorbance of a given IR band, the absorption coefficient and the effective thickness which itself is a function of the layer thickness d, respectively.[11, 12] We should mention at this point, that advantageously our multilayer system is thicker than the depth of penetration, so that changes in the thickness d (1) are not detected any more by the evanescent wave. Here the initial state is given by the multilayer in contact to pure water (0% EtOH), whose band areas (A_0) we have used for normalization aiming at a proper comparability between bands, which have different absorption coefficients ε. Since there is an obvious increase of all polyelectrolyte IR bands by increasing the EtOH content, we conclude deswelling or compression of the whole multilayer assembly by dehydration. Significantly, the steepest increase is taken by the normalized Amide I band, indicating the

strongest deswelling of the PLL layer phases. Whereas we obtained a less steepness for the ν(C=O) and ν(COO^-) due to less deswelling or dehydration of the PAC layer phases.

pH variation of MLS composed of PLL/PAC

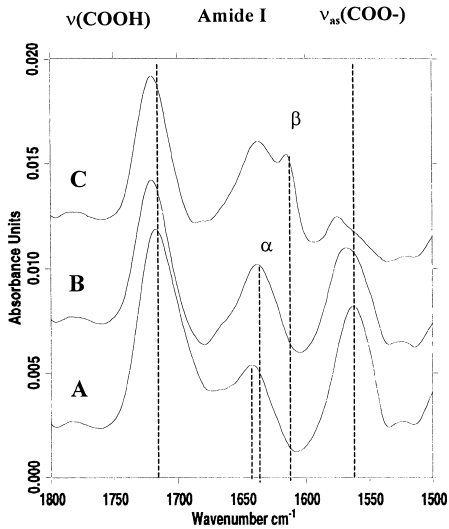

Fig. 9. *In-situ* ATR-FTIR spectra of the multilayer system PLL/PAC (MLS-20) in contact to D_2O at pD = 7.4, T = 25°C **(A),** at pD = 12, T = 25°C **(B)** , pD = 12, T = 50°C **(C)** (assignment R, α, β is given in the text).

Beside varying the composition of solvent mixtures we also applied pH variations on multilayer systems. Thereby, we were aiming at conformational changes of immobilized PLL, which initially have been reproducibly induced and studied on PLL samples in solution and analyzed by CD spectroscopy.[14] For that we have deposited a MLS-PLL/PAC-15, which was contacted to D_2O of two different pD values (7.4 and 12). Concerningly in Fig. 9 *in-situ*-ATR-FTIR spectra of MLS-PLL/PAC-15 on a Si IRE were recorded for pD = 7.4 (25°C) (A), pD = 12 (25°C) (B) and pD = 12 (50°C) (C). Complementary to CD measurements, FTIR is sensitive to the conformation of proteins and peptides, since the amide I band of the peptide units (CONH) backbone varies in position and lineshape dependent on the local environment, coupling and selection rules of the characteristic amide vibrations (amide I and II) due to

conformations α-helix, β-sheet, turn and random coil,[15-17] whereby the amide I band assignments of PLL spectra are slightly different from classical assignments.[18-20] Concerningly, at pD = 7.4 the amide I band of PLL appears at 1643 cm^{-1}, which is indicative of a random structure (R), whereas at pD = 12 the amide I band shifts to 1637 cm^{-1}, which is significant of the α-helical structure (α). Heating the PLL further to T = 50°C causes a further shift of the amide I band to 1620 cm^{-1}, which can be assigned to β-sheet structure (β). Conclusively, PLL, even incorporated in multilayers assemblies, is flexible enough to change the conformation of its backbone, like it had been shown for the dissolved state.

Binding properties of PMI/PMA multilayers

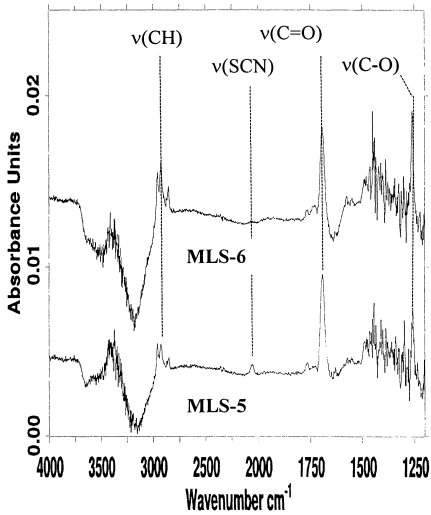

Fig. 10. ATR-FTIR spectra of MLS-5 and MLS-6 of PMI-MS/PMA-MS in the presence of 0.001m SCN solutions. From the A_{SBSR} spectra of MLS in contact to KSCN solution the A_{SBSR} spectrum of the MLS in contact to pure water was subtracted.

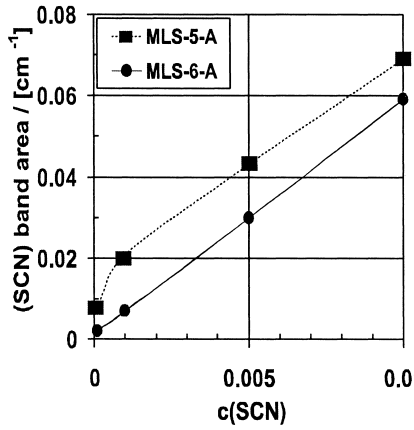

Fig. 11. Uptake of SCN^- ions by the multilayer systems MLS-5 (cubes) and MLS-6 (circles). The integrated areas of the ν(SCN) band of ATR-FTIR spectra recorded on MLS in contact to various concentrations of the KSCN solution are plotted.

To illlustrate principally the binding properties of polyelectrolyte MLS, adsorbing species of different molecular scales were studied. We started with rhodanide anions (SCN^-), which could conveniently be detected by the C≡N triple bond band at around 2100 cm^{-1}. We have

chosen the PMI-MS/PMA-MS system, whereby the PMI-MS had been synthesized directly by polymer analogous reaction from the PMA-MS polymer, since we expect an optimized charge matching between polycations and polyanions of equally linear charge density. In order to evaluate the influence of the last adsorbed PEL layer (ii) on the binding of rhodanide anions, the MLS-5 of PMI-MS/PMA-MS and the respective MLS-6 were exposed to increasingly concentrated KSCN solutions from 0.0001, 0.001, 0.005 until 0.01m. Accordingly, in Fig. 10 ATR-FTIR spectra of the MLS-5 and MLS-6 in contact to a 0.001m KSCN solution are shown in the 4000-1200 cm^{-1} range. As prominent IR bands the ν(CH), the ν(SCN) due to SCN^- ions in vicinity to the surface, the ν(C=O) due to the imide groups of PMI-MS and the ν(C-O) due to the COOH groups of PMA-MS are visible. The integrated intensities of the ν(SCN) (2100 - 2000 cm^{-1}, tight baseline), which is a direct measure of the uptake of the SCN^- ions at the MLS, were plotted against c(SCN), which is shown in Fig. 11. Qualitatively, there was a higher SCN^- uptake for the polycation terminated (MLS-5) compared to the polyanion terminated (MLS-6) multilayer.

For the quantitative determination of the adsorbed amount in case of such high bulk concentrations, one has to take into account that the evanescent field E senses both the SCN^- ions stemming from the bulk solution and the SCN^- ions concentrated or adsorbed at a certain zone above the internally reflecting surface. Therefore, the measured integrated absorbance $A_{tot} = A_{bulk} + A_{surface}$ has two contributions. A_{bulk} represents the contribution, scaling linearly with the increasing bulk SCN^- concentration c (2), whereas $A_{surface}$ is related to the nonlinearly scaling surface concentration Γ. Empirically, $A_{surface}$ might be described by a Langmuir type function (3), which roughly describes the SCN^- binding at the MLS surface.

$$A_{bulk} = a_1 \cdot c \tag{2}$$

$$A_{surface} = a_2 \cdot c/(a_3+c) \tag{3}$$

Thereby, a_1 substitutes $\varepsilon \cdot d_e$ in eq. 1, and a_2, a_3 are the empirical Langmuir constants. The parameters a_1, a_2 and a_3 can be obtained by least square fitting of the concentration versus ν(SCN) band area (integral) data by the analytical function $A_{tot} = A_{bulk} + A_{surface}$, which is summarized in Tab. 2. As a consistency check, a_1 should have the same value in the case of SCN^- binding to both MLS-5 and MLS-6, which is approximately the case (5.1 and 5.7, respectively). a_2 scales with the bound SCN^- amount and furthermore a_3 scales with the ratio of the kinetic constants of desorption and adsorption ($a_3 = k_d/k_a$),[21] which should be

understood 'semiquantitatively' being aware that four data points are fitted by a three parameter function.

Comparing now MLS-5 (a_2 = 0.018) and MLS-6 (a_2 = 0.0016), we conclude that the SCN^- uptake at the odd MLS is significantly higher compared to that of the even MLS, which is due to the attractive and repulsive electrostatic attraction forces between outermost multilayer and rhodanide anions. Ratioing the respective a_2 values according to $Q_{SCN} = a_2(MLS\text{-}5)/a_2(MLS\text{-}6)$ leads to a Q_{SCN} value of 11, which may be used as a parameter to describe the binding selectivity of this multilayer system towards SCN^- ions.

Table 2. Parameters a_1, a_2 and a_3 for the SCN^- binding at the MLS-5 and MLS-6 computed by least square fitting of the experimental concentration versus ν(SCN) integral (Fig. 11) by the sum of equation (2) and (3). (The absolute errors of the computation are further given.)

	a_1	a_2	a_3
MLS-5	5.12 ± 0.02	0.0180 ± 0.0002	0.00014 ± 0.00001
MLS-6	5.72 ± 0.07	0.0016 ± 0.0005	0.00001 ± 0.00001

Furthermore, to check the a_1 parameter, additional ATR-FTIR spectra of KSCN solutions of concentrations c = 0.0001, 0.001, 0.005 and 0.01 exposed to a naked Si plate were recorded, from whose concentration versus ν(SCN) integral data an a_1 parameter of about 5.5 was determined by least square fitting due to equation (2), which supports conveniently the a_1 values of Table 2.

Binding of oleate at MLS-PEI/PAC

In analogy to the rhodanide binding experiments, odd and even numbered multilayers of PEI/PAC were exposed to solutions of the sodium salt of oleic acid (sodium oleate) as a further higher molecular scaled negatively charged analyte. Concerningly, in Fig. 12. ATR-FTIR spectra of the MLS-5 and MLS-6 of PEI/PAC during the exposure to a 0.001m sodium oleate solution are given. Again evidently, there is higher binding of the negatively charged surfactant oleate to the MLS with the topmost PEI layer (MLS-5) and lower to the MLS with the topmost PAC layer (MLS-6). In Fig. 13. the integrated ares A_{CH} of the $\nu_s(CH_2)$ due to the CH_2 moieties of oleate are given. Analogously to the rhodanide anions at MLS in the previous section, a selectivity parameter Q_{oleate} can be determined. Thereby, differently to the SCN^- binding experiments, the oleate concentration (c = 0.001m) in the bulk phase was so small,

that no contribution to the measured $\nu_s(CH_2)$ integral, due to surface bound oleate, had to be considered. Therefore, here Q_{oleate} was determined by ratioing A_{CH} measured for MLS-5 and for MLS-6 in the presence of 0.001m sodium oleate after an adsorption time of 50 minutes, respectively, according to A_{CH}(MLS-5) / A_{CH}(MLS-6). Hence, the determined value of Q_{oleate}= 17, describes the binding selectivity of the MLS-PEI/PAC towards oleate. Interesting applications of this type of measurements could be the screening of commercial surfactants (anionic and cationic) due to their physisorption at relevant model multilayer systems (charge modified cellulose).

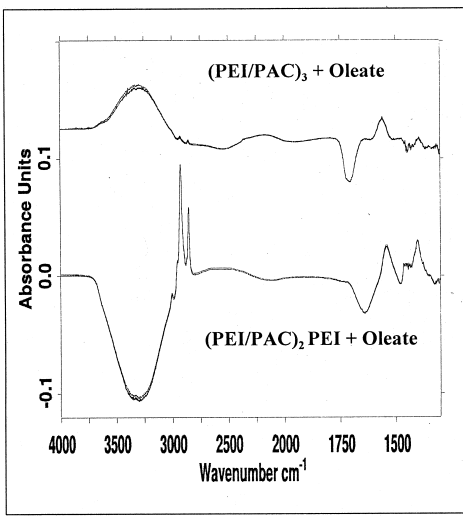

Fig. 12. ATR-FTIR spectra of the PEI/PAC multilayers MLS-5 (bottom) and MLS-6 (top) in contact to a 0.001m sodium oleate solution.

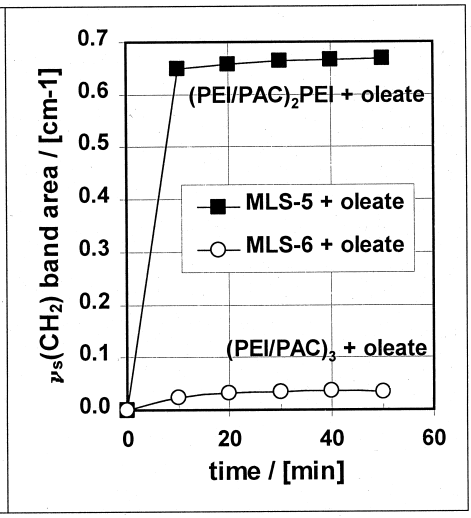

Fig. 13. Time dependent adsorption of oleate at MLS-5 and MLS-6 of PEI/PAC, rationalized by the integrated ares of the ν(CH) band due to the CH_2 moieties of oleate.

CONCLUSION

Conclusively, multilayers are easy to handle, stable and tunable model systems, which serve for fundamental and applied studies. In this paper we addressed two aspects, which is the regulation of the surface charge by the last layer (i) as well as the stimulation of the bulk phase of multilayers by aqueous mixtures of organic solvents or by pH (ii).

We have shown, that multilayers are highly selective for a variety of charged analytes. Thereby the affinity could be controlled by the choice of the last adsorbed polymer layer, which should be interesting for many applications, such as sensor sytems. In comparison to earlier studies on proteins we have presented here data on rhodanide anions and oleate to multilayers ending up either by polycation or polynion. A selectivity parameter Q was defined as the ratio between the adsorbed amount obtained at the negatively charged and that at the positively charged surface, respectively. For rhodanide at PMI-MS/PMA-MS multilayers we obtained $Q_{SCN} = 11$ and for oleate at PEI/PAC multilayers we obtained $Q_{oleate} = 17$.

Swelling experiments on multilayer assemblies of PLL and PAC exposed to mixtures of ethanol/water (10 - 70% EtOH content) gave evidence, that the PLL layers showed a more significant increase in density than the PAC layers. Additionally, pH dependent measurements have shown, that the conformation of PLL, even incorporated into multilayers, could be changed significantly.

ACKNOWLEDGEMENT

This work was partly supported by the Deutsche Forschungsgemeinschaft (SFB 287).
We thank Mr. B. Kessler for the skillful technical support.

REFERENCES

1. J. Sagiv, *J. Am. Chem. Soc.*, 102, 92 (1980)
2. A. Ulman, An Introduction to Ultrathin Organic Films: From Langmuir-Blodgett to Self-Assembly, Academic Press, New York (1999) and: A. Ulman, *Chem. Rev.*, 96, 1533 (1996)
3. R. G. Nuzzo, D. L. Allara, *J. Am. Chem. Soc.*, 105, 4481 (1983)
4. I. Mäge, E. Jähne, A. Henke, H.-J. P. Adler, C. Bram, C. Jung, M. Stratmann, *Progress in organic Coatings*, 1998, 34, 1-12
5. G. Decher, J. D. Hong and J. Schmitt, *Thin Solid Films*, 210/211, 831 (1992)
6. P. Bertrand, A. Jonas, A. Laschewsky, R. Legras, *Macromol. Rapid Commun*, 21, 319-348 (2000)
7. M. Müller, T. Rieser, K. Lunkwitz, S. Berwald, J. Meier-Haack, D. Jehnichen, *Macromol. Rapid Commun.* 19 (7), 333-336 (1998)
8. M. Müller, T. Rieser, K. Lunkwitz, J. Meier Haack, *Macromol. Rapid Commun*, 20 (12), 607-611 (1999)

9. M. Müller, M. Brišš ová, T. Rieser, A. C. Powers and K. Lunkwitz, *Materials Science & Enginieering* C, 8-9, 167-173 (1999)
10. J. Meier-Haack, W. Lenk, D. Lehmann, K. Lunkwitz, *J. Membr. Sci.* (submitted)
11. N. J. Harrick, Internal reflection Spectroscopy, Harrick, Ossining, New York (1967)
12. U.P. Fringeli, in ´Encyclopedia of Spectroscopy and Spectrometry´, J.C. Lindon, G.E. Tranter, J.L.Holmes (eds), Academic Press, 2000; U. P. Fringeli, *Chimia*, 46, 200-214 (1992)
13. to be published
14. N. Greenfield, G. D. Fasman, *Biochemistry*, 8 (10), 4108-4116 (1969)
15. A. Elliott, E. J. Ambrose, *Nature*, 165, 921 (1950)
16. T. Miyazawa, *J. Chem. Phys.*, 32, 1647 (1960)
17. M. Byler, H. Susi, *Biopolymers*, 25, 469 (1986)
18. Y. N. Chirgadze and E. V. Brazhnikov, *Biopolymers*, 13, 1701-1712 (1974)
19. M. Jackson, P. I. Haris and D. Chapman, *Biochem. Biophys. Acta*, 998, 75-79 (1989)
20. M. Müller, R. Buchet and U. P. Fringeli, *J. Phys. Chem.*, 100 (25), 10810-25 (1996)
21. M. Schöpflin, U. P. Fringeli, X. Perlia, *J. Am. Chem. Soc.*, 109, 2375 (1987)